SUPPLEMENTAL MATERIAL

DETAILED METHODS

CHF Model Validation. The CHF model was validated in 10 consecutive dogs with respect to its effect on left ventricular and left atrial size. These data, as seen in Supplemental Figure 1, show that there is a progressive increase in left atrial volume (LA Vol), left ventricular end diastolic diameter (LVEDD), and left ventricular end systolic diameter (LVESD) with rapid right ventricular pacing.

Supplemental Figure 1.

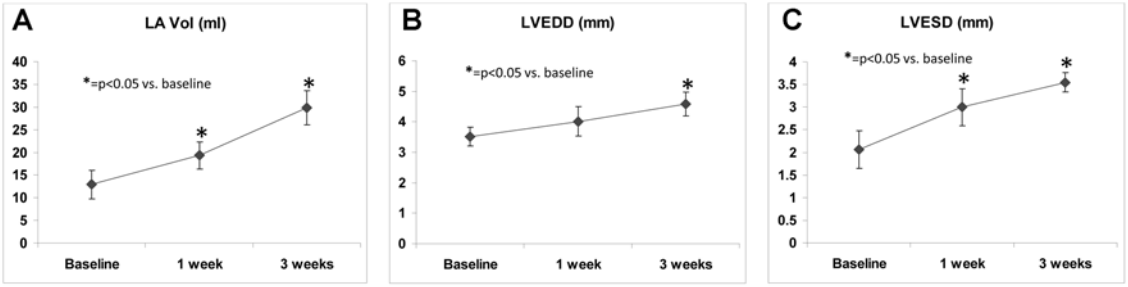

Effective Refractory Periods. For each ERP, the pacing protocol consisted of a drive train (S1) of eight beats with a cycle length of 400 ms followed by an extrastimulus (S2). The S2 was decremented by 10 ms until loss of capture. The longest S2 which did not capture was considered the ERP for that particular site. Pacing was performed at an output current twice the threshold required for consistent capture of the tissue. The mean ERP was used as the representative ERP for each of the three sites as well as the entire left atrium.

Atrial Fibrillation Sustainability and Dominant Frequency. Current was set at four times the threshold for capture. The maximum durations of the AF episodes induced by the burst pacing were calculated for each intervention.
Electrograms were pre-processed with 40 to 250 Hz band pass filtering, rectification, and 20 Hz low pass filtering.[1] Power spectra of the processed electrograms were obtained using the Fast Fourier Transform. The DF, defined as the frequency with the highest power in the power spectrum, was used as the estimation of the local AF activation rate.[2] A composite DF from each region was calculated by averaging the values spatially across all channels of the plaque and temporally across the four four-second segments.[2]

Activation Mapping. Activation times for each electrode recording for a specific paced beat were selected at the peak voltage of the bipolar electrograms after band pass filtering (40 to 250 Hz), rectification, and low pass filtering (20 Hz). The filtering and rectification steps were used to account for the different morphologies of bipolar electrogram recordings.[3, 4] Two-dimensional activation maps for the PLA and LAA were then constructed from the activation times.

The left panel of the Supplemental Figure 2 shows an example of raw electrograms of one sinus beat obtained from the PLA. The middle panel shows the electrograms after band pass filtering, rectification, and low pass filtering. The dots indicate the detected peaks of the processed electrograms. The right panel shows the activation map constructed with the activations times determined from the second panel. The isochrones, indicated by the white lines, show the progression of the wavefront every 3 milliseconds.

Supplemental Figure 2.

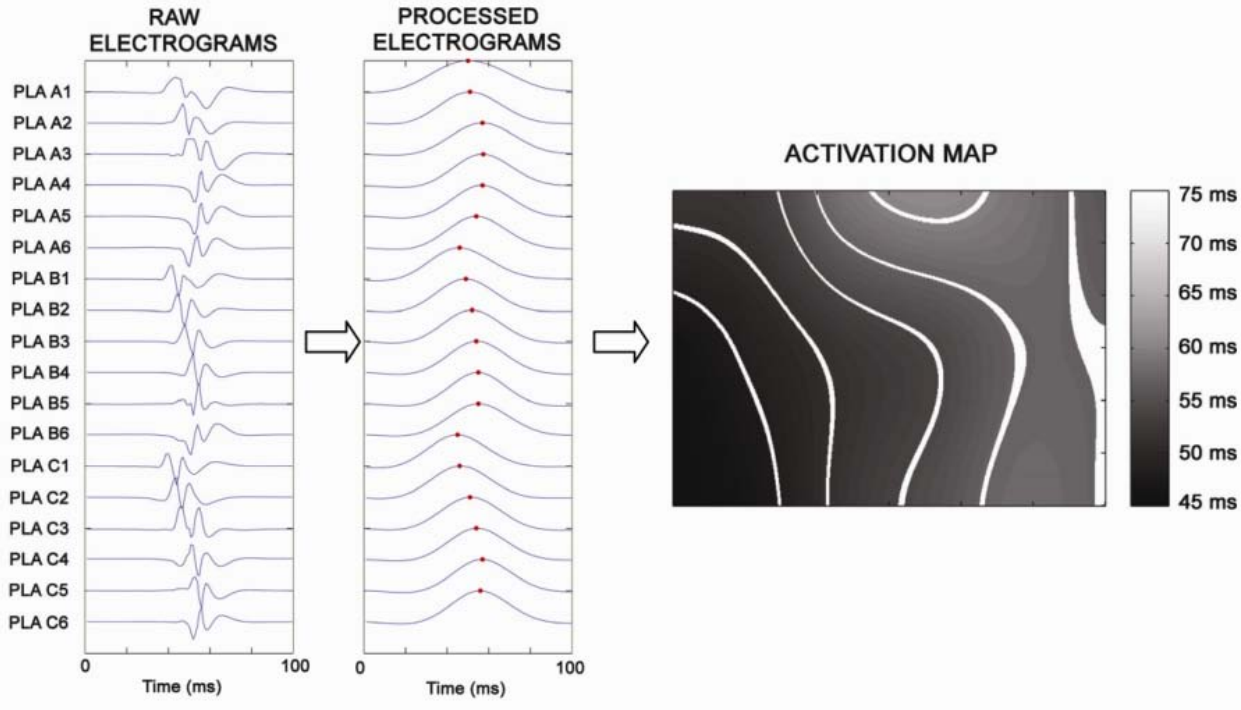

Good reproducibility of the baseline and atropine maps was evident with high correlation coefficients of activation times for both the normal (PLA: 0.981±0.005, LAA: 0.985±0.004) and CHF (PLA: 0.977±0.003, LAA: 0.970±0.007) dogs. There was also good reproducibility of the baseline and propranolol maps evident by the high correlation coefficients for both normal (PLA: 0.968±0.007, LAA: 0.992±0.001) and CHF (PLA: 0.963±0.009, LAA: 0.966±0.009) dogs.

Tissue Sample Preparation. For both normal and CHF dogs, immediately following the termination of the *in vivo* electrophysiology assays, the heart was promptly excised out of the chest and immersed in ice-cold cardioplegia solution containing (mmol/L) NaCl 128, KCl 15, HEPES 10, $MgSO_4$ 1.2, NaH_2PO_4 0.6, $CaCl_2$ 1.0, glucose 10, and heparin (0.0001 U/mL); pH 7.4. The heart was quickly cannulated via the aorta and perfused with ice cold cardioplegia solution containing protease inhibitors (Sigma cocktail cat#P8340) until vessels were clear of blood and tissue was cold. The atria were separated from the associated ventricles, and tissue samples were taken from the PLA, PV, and LAA regions of the left atrium and snap frozen in liquid nitrogen, and subsequently stored at -80° C.

Immunohistochemistry. Immunohistochemistry was performed to examine the anatomy of the parasympathetic and sympathetic nerves in the atria. For the PVs, cross sections were cut serially from proximal to distal. The sections from the PLA and LAA were cut parallel to the plane of the mitral annulus as to include both the epicardial and endocardial aspect of the myocardium in each slice. Sections were air-dried and fixed in acetone for ten minutes before being washed in Tris-buffered saline (TBS). Hydrogen peroxidase block (Dako, Carpenteria, CA) was placed on the sections for ten minutes, and the slides were washed in TBS. Protein block was placed on the sections for thirty minutes. Primary antibodies were then incubated overnight at 4°C. Antibodies for dopamine β-hydroxylase (DBH; Chemicon, Temecula, CA) were used to stain sympathetic nerves, whereas antibodies for acetylcholinesterase (AChE; Millipore;) were used to stain parasympathetic nerves. The specificity of

DBH for sympathetic nerve fibers was confirmed by the use of a sympathetic nerve marker, i.e., tyrosine hydroxylase (TH; Chemicon), which stained the same nerve elements that were stained by DBH. Similarly, the specificity of parasympathetic staining was confirmed using a second parasympathetic nerve marker, i.e., cholineacetyl transferase (ChAT; Chemicon), which stained the same nerve elements that were stained by AChE. Some sections were double-stained for AChE and DBH. After incubation, the slides were washed in TBS, and the appropriate secondary antibody (Chemicon) was placed on the sections for 30 min. The sections were again washed in TBS, and the appropriate chromagen was added to each specimen. Sympathetic nerves were stained blue with 5-bromo-4-chloro-3-indolyl phosphate (BCIP), and parasympathetic nerves were stained brown with 3,3'-diaminobenzidine (DAB). Cell nuclei were marked by placement of the specimens in methyl green (Dako) for 10 min. The specimens were then dehydrated in alcohol, mounted, and examined under light microscopy. Cardiac ganglia were defined as nerve bundles containing one or more neuronal cell bodies. The presence of neuronal cell bodies within nerve bundles was confirmed by staining these bundles for hematoxylin; all neuronal cell bodies stained positive for hematoxylin, thereby excluding the presence of fat cells within these bundles. Specimens taken from the cervical vagus nerve served as a positive control for parasympathetic nerve fibers but a negative control for sympathetic nerves. Specimens from the stellate ganglia served as a positive control for sympathetic fibers but a negative control for parasympathetic nerve fibers. Quantification was performed manually with a light microscope. Mean densities (number per mm^2) of nerve bundles and cardiac ganglia cells were quantified using 1x1 mm grids at 10 times magnification. We also counted the number of parasympathetic and sympathetic fibers within individual nerve bundles. Sizes of nerve bundles were quantified using rectangular 1x1 mm grids at 20 times magnification.

Densities of muscarinic and beta-adrenergic receptors. The βAR binding assays were performed in duplicate at 37˚C for one hour in 250 μL of binding buffer containing 50 to 100 μg of membrane proteins and increasing concentrations of 125I-iodocyanopindolol (0.01 to 1 nmol/L) in the absence or presence of either Betaxolol (β_1-antagonist; 1 μmol/L) or ICI-118,551 (β_2-antagonist; 1 μmol/L). Following incubation, 4 ml ice-cold buffer was added to the reaction mixture and rapidly filtered under vacuum on GF/C filters. The filters were washed with 4 x 5 ml of ice-cold buffer, air dried and radioactivity was counted in gamma counter. The specific counts were obtained by subtracting non specific counts from total counts. The receptor density (B_{max}) was determined from Scatchard plots. For MRs, the experiments were same as described above except 3H-quinuclidynl benzilate (1 to 20 nmol/L) was used as radioligand and atropine sulfate (1 μmol/L) as the competitive cold ligand. The air dried GF/C filters were counted in scintillation counter with 5 ml scintillation fluid.

AChE activity. The Ellman's method acetylcholinesterase hydrolysis products are detected at 412 nm absorbance, which was read every 2min for 30min via UV-VIS spectrophotometer (BioRad microplate reader). Absorbance was plotted against time and enzyme activity was calculated from the slope of the line so obtained and expressed as a percentage compared to an assay using a buffer without an inhibitor.

Isoproteronol effect on ERPs. The ERP shortening due to sympathetic stimulation with isoproterenol compared to propranolol was not significantly different between CHF and normals (Supplemental Figure 3).

Supplemental Figure 3.

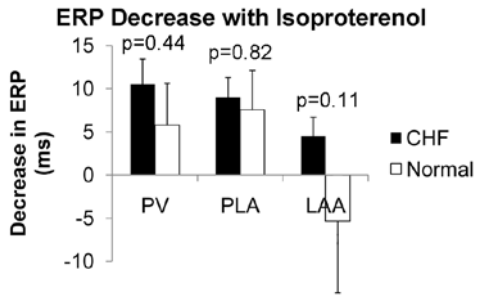

Vagal Stimulation effect on ERPs with and without physostigmine in normal dogs. The decrease in ERP from vagal stimulation with physostigmine was not different from the decrease in ERP from vagal stimulation at baseline for normal dogs (Supplemental Figure 4). This is in contrast with CHF dogs where the ERP decrease from vagal stimulation was significantly more with physostigmine than at baseline (see main manuscript). This finding is consistent with the increase in AChE with CHF.

Supplemental Figure 4.

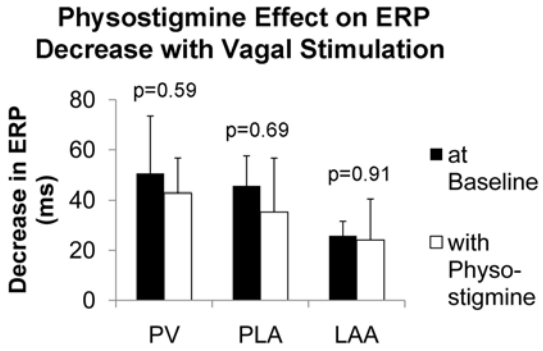

Carbachol effect on ERPs. The shortening of ERPs due to application of 1 mmol/L Carbachol (CCh) to the PLA was not significantly different between CHF and normal (Supplemental Figure 5). Thus, it can be concluded that M_2R desensitization was not responsible for the decrease in vagal-induced ERP shortening.

Supplemental Figure 5.

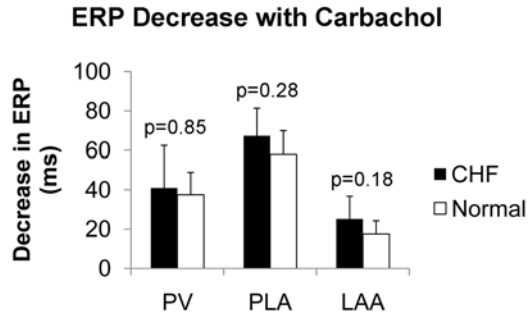

REFERENCES

1. Arora R, Ng J, Ulphani J, Mylonas I, Subacius H, Shade G, Gordon D, Morris A, He X, Lu Y, Belin R, Goldberger JJ, Kadish AH. Unique autonomic profile of the pulmonary veins and posterior left atrium. *Journal of the American College of Cardiology.* 2007;49(12):1340-1348.

2. Ng J, Kadish AH, Goldberger JJ. Effect of electrogram characteristics on the relationship of dominant frequency to atrial activation rate in atrial fibrillation. *Heart Rhythm.* 2006;13:1295-1305.

3. Botteron GW, Smith JM. A technique for measurement of the extent of spatial organization of atrial activation during atrial fibrillation in the intact human heart. *IEEE Trans Biomed Eng.* 1995;42:579-586.

4. Botteron GW, Smith JM. Quantitative assessment of the spatial organization of atrial fibrillation in the intact human heart. *Circulation.* 1996;93:513-518.